



Published in final edited form as:

*J Immunother.* 2013 ; 36(9): 477–489. doi:10.1097/01.cji.0000436722.46675.4a.

## Immunogenicity of murine solid tumor models as a defining feature of *in vivo* behavior and response to immunotherapy

Melissa G. Lechner<sup>1</sup>, Saman S. Karimi<sup>1</sup>, Keegan Barry-Holson<sup>1</sup>, Trevor E. Angell<sup>2</sup>, Katherine A. Murphy<sup>3</sup>, Connor H. Church<sup>1</sup>, John R. Ohlfest<sup>3</sup>, Peisheng Hu<sup>1</sup>, and Alan L. Epstein<sup>1</sup>

<sup>1</sup>Department of Pathology, Keck School of Medicine, University of Southern California, Los Angeles, California

<sup>2</sup>Department of Medicine, Keck School of Medicine, University of Southern California, Los Angeles, California

<sup>3</sup>Departments of Pediatrics and Neurosurgery, University of Minnesota, Minneapolis, Minnesota

### Abstract

Immune profiling has been widely used to probe mechanisms of immune escape in cancer and identify novel targets for therapy. Two emerging uses of immune signatures are identification of likely responders to immunotherapy regimens among individuals with cancer or to understand the variable responses seen among subjects with cancer in immunotherapy trials. Here the immune profiles of six murine solid tumor models (CT26, 4T1, MAD109, RENCA, LLC, and B16) were correlated to tumor regression and survival in response to two immunotherapy regimens. Comprehensive profiles for each model were generated using quantitative RT-PCR, immunohistochemistry, and flow cytometry techniques, as well as functional studies of suppressor cell populations (Treg and MDSC), to analyze intratumoral and draining lymphoid tissues. Tumors stratified as highly or poorly immunogenic, with highly immunogenic tumors showing significantly greater presence of T-cell co-stimulatory molecules and immunosuppression in the tumor microenvironment. An absence of tumor-infiltrating CTL and mature DC was seen across all models. Delayed tumor growth and increased survival with suppressor cell inhibition and tumor-targeted chemokine +/- DC vaccine immunotherapy was associated with high tumor immunogenicity in these models. Tumor MHC class I expression correlated with overall tumor immunogenicity level and was a singular marker to predict immunotherapy response with these regimens. By using experimental tumor models as surrogates for human cancers, these studies demonstrate how select features of an immune profile may be utilized to identify patients most likely to respond to immunotherapy regimens.

### Keywords

Experimental tumor models; immunotherapy; MHC class I; immunogenicity; suppressor cells

### INTRODUCTION

Tumor-host immune interactions are increasingly recognized as significant influences on tumor progression and patient prognosis [1–3]. Successful immunotherapy promises

Correspondence: Alan L. Epstein, MD, PhD; 2011 Zonal Ave., HMR 205, Los Angeles, California 90033; aepstein@usc.edu; phone: 323-442-1172; fax: 323-442-3049.

**Financial Disclosure:** All other authors have no conflicts of interest to declare.

significant advances over conventional treatment modalities by utilizing the inherent specificity, systemic trafficking, and memory of the host adaptive immune system [4]. Clinical experiences with immunotherapy to date have highlighted the need for different paradigms in patient selection, assessing tumor response to therapy, and monitoring for adverse events [5,6]. Notably, while immunotherapy can produce durable and complete regressions, the sporadic successes of immunotherapy and the observed toxicities of many regimens highlight the need for better ways to identify the subset of patients most likely to respond to treatment [7–12]. Moreover, disease anatomic spread (TNM classification) and histology traditionally used to determine patient prognosis are of limited use in regards to immunotherapy [3,13].

Challenges to successful immunotherapy are the complexity of the immune system and the diversity of strategies used by tumors to escape host immunity [14]. Cancer cells may evade the immune system by resemblance to self and loss of immunogenicity (*e.g.* deletion of tumor-associated antigens and MHC down-regulation) [15,16]. Tumors retaining immunogenicity may overcome host immune surveillance by the expression of inhibitory immune ligands [*e.g.* programmed death ligand (PDL) 1, cytotoxic T-lymphocyte antigen (CTLA)-4], suppressive cytokines [*e.g.* interleukin (IL)-10, transforming growth factor (TGF) $\beta$ ], and the recruitment of suppressor cell populations, including regulatory T cells (Treg), myeloid-derived suppressor cells (MDSC), and Type II tumor-associated macrophages (TAM) [4,14]. Previously, we showed that the immune milieu of breast and colorectal cancer patients varied significantly both between cancer type and tumor stage, and suggested that this may account for the sporadic results achieved with immunotherapy in cancer treatment [17]. Immune profiling has identified peritumoral and intratumoral immune populations as indicators of recurrence and overall survival in a number of cancers [1,18–20]. However, little is known about how the pre-treatment immune profile of a tumor might predict the response to immunotherapy regimens. Two emerging uses of immune signatures are identification of likely responders to immunotherapy regimens among individuals with cancer or to understand the variable responses seen among subjects with cancer in immunotherapy trials. This report is the culmination of many years of work to define the tumor-host immune interactions in six commonly-used murine tumor models, including comprehensive and comparative studies of their immunogenicity and ability to induce immune suppression. Furthermore, these data were then correlated with the results of two immunotherapy treatments as a demonstration of how critical features within the immune profile can predict response to immunotherapy. In this regard, we believe that this germinal work will provide investigators with a foundation for understanding the immunologic behavior of these tumor models and their best use in subsequent immunotherapy experiments.

## MATERIALS AND METHODS

### Cell lines and animals

All cell lines were obtained from the American Type Culture Collection [(ATCC), with authentication by short tandem repeat] and maintained in complete medium as described previously [21]. Tumors were grown in mice using two different approaches, described in detail previously [7,17,22,23]. Briefly, “transplantable tumors” were generated by subcutaneous (CT26, 4T1, MAD109, RENCA, LLC, or B16) or intracerebral (GL261, ONC26M4) inoculation of tumor cell lines into adult female mice, with tumors developing over days [22]. These tumors were grown in syngeneic, immunocompetent mouse strains, specifically CT26, 4T1, MAD109, and RENCA in BALB/c mice, LLC, B16, and GL261 in C57BL/6 mice, and ONC26M4 in FVBN mice. “Spontaneous tumors” were generated by intracerebral injection of DNA plasmids encoding three oncogenes and a firefly luciferase

reporter [pT2/C-Luc//PGK-SB13 (0.07  $\mu\text{g}$ ), pT/CAGGS-NRASV12 (0.14  $\mu\text{g}$ ), and pT2/shP53/GFP4/mPDGF (0.14  $\mu\text{g}$ )] into neonatal C57BL/6 or FVBN mice to transform endogenous brain cells [22,23]. Growth of gliomas was monitored by bioluminescence imaging, as described previously [22]. Growth of subcutaneous tumors was monitored by caliper measurements in three dimensions every 2–3 days. For all studies of subcutaneous transplantable tumor models (CT26, MAD109, 4T1, RENCA, B16, and LLC), except those studies explicitly comparing early and late tumors, tumor specimens and accompanying lymphoid tissues were collected from groups of mice when tumors reached 1cm in diameter (tumor volume 300–600mm<sup>3</sup>). Institutional Animal Care and Use Committee-approved protocols were followed.

### Quantitative reverse transcriptase polymerase chain reaction (qRT-PCR)

RNA was isolated from fresh-frozen tumor sections or syngeneic naïve mouse subcutaneous control tissue and amplified for qRT-PCR in triplicate as described previously [22] using primers from the NIH qRT-PCR primer database (mouseprimerdepot.nih.gov). Gene expression was calculated as a percent of GAPDH and mean fold change relative to naïve syngeneic mouse subcutaneous tissue was determined.

### Immunohistochemistry

Tumors and tumor-draining lymph nodes (TDLN) collected were formalin-fixed paraffin-embedded (FFPE) or liquid nitrogen flash-frozen OTC-embedded tissue sections and stained using standard immunohistochemistry (IHC) techniques [24]. Tumor infiltrating leukocytes (TIL) were quantified as the average number of positive cells (Supplemental Figure 1) across 2–3 HPF (400 $\times$ ) for each of 3 tumor sections of each model. Areas of necrosis or hemorrhage, identified on corresponding H&E-stained sections, were excluded from TIL scoring and two blinded individuals scored each section. Image acquisition was as previously described [20].

### Flow cytometry

Groups of tumor bearing mice were sacrificed at early (tumor volume 40–60mm<sup>3</sup>) or late (tumor volume 800–1000mm<sup>3</sup>) time points. Syngeneic naïve mice were analyzed in parallel. Single-cell suspensions were generated from fresh spleen, TDLN, and tumor specimens by mechanical dissociation and passage through a 70 $\mu\text{m}$  filter. Cells were stained with fluorescence-conjugated monoclonal antibodies or isotype controls, as described previously [21]. Samples were run (20,000 events) in duplicate on a BD LSR II flow cytometer using FACSDiva software (BD) for acquisition and compensation and analyzed using FlowJo software (FlowJo).

### Suppression assays

Treg and MDSC were isolated from tumors, spleens, and TDLN of tumor-bearing mice using the mouse CD4<sup>+</sup> CD25<sup>+</sup> Regulatory T Cell and Myeloid-Derived Suppressor Cell (Gr-1<sup>high</sup>Ly-6G<sup>+</sup> and Gr-1<sup>dim</sup>Ly-6G<sup>-</sup>) isolation kits (Miltenyi Biotec), respectively. Suppressor cells were cultured at variable ratios (1:1 to 1:20) with CFSE-labeled (3 $\mu\text{M}$ ) fresh mononuclear spleen cells from syngeneic naïve mice in the presence of CD3/CD28 beads (Invitrogen). Spleen cell proliferation was analyzed after four days on a BD LSR II flow cytometer as described above.

### Immunotherapy studies

BALB/c or C57BL/6 mice bearing syngeneic tumors were randomized into groups (n=5) for treatment when tumor volumes reached 40–80mm<sup>3</sup>. Groups of mice received no treatment (PBS vehicle only) or one of two immunotherapy regimens previously used in our laboratory (Figure 5). Regimen 1 contained low-dose chemotherapy and tumor-targeted

chemokine LEC (LEC/chTNT-3) fusion protein and Regimen 2 contained these components as well as a dendritic cell vaccine and toll-like receptor agonist. Of the two regimens, Regimen 2 was considered more immune stimulating and was shown to more frequently induce autoimmunity. Chemotherapy reagents 5-fluorouracil [(5-FU), 50mg/kg, Sigma] and cyclophosphamide [(CTX), 50mg/kg, Sigma] were dissolved in sterile PBS and injected intraperitoneally (*i.p.*) on treatment day 0. CD11c<sup>+</sup> bone marrow-derived dendritic cells (DC) were generated by 7-day culture in GM-CSF and IL-4 and subsequent positive magnetic bead isolation (Miltenyi Biotec). For tumor vaccine preparation, these DC were cultured overnight with irradiated (10,000rads) tumor cells (2:1 ratio), Poly I:C/L:C Hiltonol (5µg/mL, Oncovir), and GM-CSF and IL-4 (10ng/mL, R&D systems). For vaccination, 1×10<sup>6</sup> DC were injected *i.p.* with 30µg Hiltonol in 200µl PBS per mouse, ipsilateral with the tumor. The LEC/chTNT-3 fusion protein [25,26] was given as an *i.p.* injection of 30µg/dose in 100µl of PBS. Mouse tumor volumes were measured every 2–3 days by caliper and mice were sacrificed when tumor volumes reached 2cm in diameter or when animal morbidity mandated sacrifice under institutional vivarium protocols.

### Statistical Analyses

Differences in mean fold change of immune-related gene expression and TIL counts were compared among models by ANOVA and between highly and poorly immunogenic models by Student t tests, with correction for multiple comparisons using the Holm-Sidak method. Differences in mean splenocyte proliferation in suppression assays were evaluated by ANOVA then Dunnett's test for pair-wise comparisons. Tumor growth rates were estimated by linear regression analysis. Differences in tumor volume among untreated and treated groups were evaluated by ANOVA then Dunnett's test for pairwise comparisons, while differences in animal survival were evaluated by log-rank test. All tests were conducted with Prism 6 software (GraphPad Software, Inc). P<0.05 was considered statistically significant.

## RESULTS

### Tumor models segregate as strongly versus poorly immunogenic by gene expression

Six commonly-used murine solid tumor models demonstrated diverse tumor-host immune interactions. Immune-related gene expression in tumor specimens of CT26 colon, 4T1 breast, RENCA renal cell, and MAD109 lung models, syngeneic in BALB/c, and LLC lung and B16 melanoma models, syngeneic in C57BL/6, was measured by qRT-PCR. Twenty-seven genes were included in the final immune profile panel, including markers of immune cell populations, indicators of dendritic cell and T-cell activation, mediators of immune suppression, and microenvironment and vasculature-related factors, as shown in Figure 1A. By analysis of RNA from the whole tumor specimen, these studies capture the immune response and the immune dysfunction generated by the tumor in infiltrating host immune cells, as well as the immune adaptation expressed by the tumor cells themselves. The most prominent difference was the extent of immune activation or immunogenicity among tumor models.

Two distinct patterns of immune alteration were observed: strongly immunogenic tumors with up-regulation of many immune activation genes (*e.g.* CT26, RENCA, 4T1) and poorly immunogenic tumors with generalized down-regulation of immune-related gene expression (*e.g.* MAD109, LLC, B16). As shown in Figure 1A, highly immunogenic models had significantly different expression of numerous immune-related genes compared with poorly immunogenic models. Strongly immunogenic tumors had significant up-regulation of pan-leukocyte (*CD45*), T-cell (*CD3*, *CD4*), and myeloid cell (*CD11c*, *CD11b*) genes, suggesting the presence of immune effector cells in the tumor microenvironment. Additionally, these tumor specimens displayed increased expression of T-cell activation genes (*CD25*, *CD62L*)

and DC activation and co-stimulatory genes (*CD80*, *CD86*, *OX40L*, *GITRL*, *CD40*, *CD137L*). In contrast, tumor models at the other end of the spectrum showed general down-regulation of these genes relative to naïve syngeneic controls. This absence of immune activation in immunocompetent animals suggests that the host immune system is unaware of or indifferent to tumor cells. In the presence of a significant tumor burden, as in these experimental animals, such immunologic indifference suggests that the surviving tumor cells have evolved to evade immune detection, such as by loss of antigenic proteins and resemblance to normal self tissues. As predicted, tumor models with up-regulation of immune activation also showed the greatest increase in immune suppression related gene expression, including enzymes *indoleamine 2,3-dioxygenase (IDO)*, *arginase (ARG)-1*, and *inducible nitric oxide synthase (iNOS)*, and suppressive cytokines *TGFβ* and *IL-10*, which are known to mediate T-cell dysfunction [14, 27–29]. Inhibitory ligand *CTLA-4* was an exception to this trend, with greatest expression seen by poorly immunogenic MAD109, LLC, and B16 tumor models.

These patterns suggest two successful strategies for tumor survival in the immune competent host: 1) countering of host immune recognition and activation by tumor-mediated immune suppression or 2) evasion of host immune detection by resemblance to self and loss of antigenicity. As shown in Figure 1B, immunogenicity levels correlated directly with positivity of mouse MHC class I molecule H2-D expression on tumor cells *in vivo*.

### Tumor growth rate inversely related with level of immunogenicity

Growth of these six tumor models in immune-competent mice without treatment was variable (Figure 1C). Interestingly, tumor growth rate correlated indirectly with MHC class I expression and overall immunogenicity of the tumor model, with fastest growth in B16, LLC, and MAD109 and slowest growth in CT26, RENCA, and 4T1. All six tumor models demonstrated similar proliferation rates as determined by Ki-67 staining, suggesting that the difference in tumor growth observed *in vivo* was not the result of faster proliferation by some models (Figure 1D). Staining for caspase-3 in tumor sections revealed a trend toward increased apoptosis in the slower growing, more immunogenic tumor models but the difference was not statistically significant (data not shown).

### Comparison of spontaneous versus transplanted tumor models

The method of experimental tumor generation in animals, *i.e.* spontaneous versus transplanted disease, is an area of controversy amongst immunotherapy researchers [30]. While many researchers, like us, elect to use transplantable tumor models to facilitate faster immunotherapy studies, spontaneous tumor models could potentially produce different immune-editing and host tolerance mechanisms. Comparison of murine glioblastoma tumor models in C57BL/6 and FVBN mice strains by a similar qRT-PCR immune gene expression panel showed that the mode of tumor generation (*i.e.* spontaneous versus transplantable) had a modest influence on tumor-host immune interactions (Figure 2, Murphy *et al.*, [22]). A statistically significant difference in immune-related gene expression was observed for 1/31 genes (*ARG-1*) between FVBN models and 4/31 genes (*IFNγ*, *PDL1*, *VEGF*, *STAT3*) between C57BL/6 models. Spontaneous glioblastomas in FVBN mice also showed a strong trend toward greater expression of co-stimulatory molecules compared with the transplanted tumors. The spontaneous and transplanted models otherwise had very similar intratumoral immune profiles. Compared with naïve mice, both glioma models in C57BL/6 mice showed increased immune cell infiltrate (*CD11c*, *CD3*, *Ly6G*, *F4/80*, and *CD49b*), down-regulation of co-stimulatory genes *OX40L* and *CD40L*, up-regulation of suppressive ligands and enzymes (*ARG-1*, *IL-6*, *IL-10*, *TGFβ*, *VEGF*), and an elevation of *STAT3* gene expression. In the FVBN strain, both spontaneous and transplanted glioblastomas demonstrated up-regulation of suppressive genes *CTLA-4*, *IL-6*, *IL-10*, and *ARG-1*, decreased expression of

DC maturity genes *CD80* and *CD86*, and similar patterns of immune cell transcription factors. In these experiments, spontaneous tumors were not consistently more or less immunogenic than their transplanted equivalents.

### Marked absence of tumor-infiltrating effector cells seen in all tumor models

The extent of host immune response to tumors was measured by the number of effector cells in specimens from tumor-bearing mice using immunohistochemistry and flow cytometry (Figures 2–3, Supplemental Figures 1–2). These studies, in contrast to the above gene expression studies, were designed to examine only the responding host leukocytes in the tumor and draining lymphoid tissues, and not proteins expressed directly by the tumor cells. For immunohistochemistry, FFPE tumor tissue sections were stained with markers of immune cell populations (CD3, CD8, CD11c, CD11b, F4/80, CD45R/B220, FoxP3), co-stimulatory ligands (CD40, CD40L, OX40L, CD137L), suppression molecules (CTLA-4, ARG-1, iNOS), and cytokines (TGF $\beta$ , IL-10, IL-6, IL-1 $\beta$ ) (Supplemental Figure 1). Tumor infiltrating active T-cells (CD3<sup>+</sup> CD8a<sup>+</sup> CD107a<sup>+</sup>) and DC (CD11c<sup>+</sup> CD80<sup>+</sup>CD86<sup>+</sup>) were also measured by flow cytometry in fresh tumor specimens. These studies identified several features of immune dysfunction that were observed amongst all of these tumor models, namely an absence of tumor infiltration by cytotoxic T cells and mature dendritic cells. IHC staining demonstrated rare or absent CD8a<sup>+</sup> T-cells and CD11c<sup>+</sup> DC in established tumors in all models, even highly immunogenic CT26 (Figure 3A, Supplemental Figure 2A). Flow cytometry analysis of activated cytotoxic T cells (CD3<sup>+</sup> CD8a<sup>+</sup> CD107a<sup>+</sup>) and mature DC (CD11c<sup>+</sup> CD80<sup>+</sup> CD86<sup>+</sup>) similarly showed these cell populations to be rare or absent in the tumor, TDLN, and spleen in all models and not increased relative to naïve syngeneic controls (Figure 4). CD45R<sup>+</sup> B cells were rare in all models, but more frequent in highly immunogenic models ( $p < 0.05$ ), especially CT26 and 4T1 (Figure 3A, Supplemental Figure 2A). There is evidence to suggest that B cells in the tumor setting can help to promote T cell priming and the generation of memory T cells [31], therefore the absence of these cells may contribute to poor anti-tumor immunity. Established tumors of all models did contain significant numbers of granzyme B<sup>+</sup> cells (*e.g.* CTL and natural killer cells), though this population alone does not appear to be sufficient to produce tumor clearance. Tumor-infiltrating macrophages (F4/80<sup>+</sup>) were one of the most prevalent immune cell populations observed in the tumors, but along with CD3<sup>+</sup> T-cells and CD11b<sup>+</sup> myeloid cells, encompass both immune effectors and immune suppressor populations. Further analysis of immune suppressor ligands and directly of suppressor cell populations in these tumor models suggests that these populations include a significant suppressor cell component discussed below.

### Co-stimulatory ligand deficits greatest in poorly immunogenic tumor models

Efficient DC priming and activation of cognate T-cells is necessary to generate successful anti-tumor immune responses [7,32–34]. Expression of common co-stimulatory molecules in the tumor (Figure 1) and specifically on TIL (Figure 3B, Supplemental Figure 2B) was measured as an indicator of the extent of co-stimulation in tumor models. As expected, co-stimulatory markers OX40L, CD137L, CD40, and CD40L were more frequently present on TIL in more immunogenic tumor models CT26, RENCA, and 4T1, than in poorly immunogenic ones ( $p < 0.05$ ) (Figure 3B). Immunotherapy regimens providing exogenous co-stimulation (soluble ligand fusion proteins or agonist antibodies) may yield the most benefit in poorly immunogenic tumors. In contrast, the host immune system appears capable of generating significant T-cell co-stimulation endogenously in the most immunogenic tumor models and thus immunotherapy to reverse immune suppression and improve trafficking of effectors into the tumor may be of greater benefit for therapy in these tumors. Intratumoral gene expression and IHC data highlight specific deficits that can be targeted with immunotherapy. Examples include OX40L in RENCA, MAD109, LLC, and B16;

GITRL in 4T1, RENCA, LLC, and B16; CD40/CD40L in RENCA, MAD109, LLC, and B16; and CD137L in LLC, and B16.

### Universal presence and activity of immune suppressor cells across all tumor models

The presence and activity of suppressor cells were measured in the tumor and secondary lymphoid tissues by IHC, FACS, and suppression assays (Figures 3–4, Supplemental Figure 2C). TIL in highly immunogenic tumor models displayed significantly greater levels of FoxP3 (especially in CT26), CTLA-4, ARG-1, and iNOS ( $p < 0.05$  for all) than poorly immunogenic models. Flow cytometry of CD4<sup>+</sup>CD25<sup>+</sup>FoxP3<sup>+</sup> Treg and CD11b<sup>+</sup>Gr-1<sup>+</sup> MDSC in tumors, TDLN, and spleens of mice showed modest increases or no changes in the quantities of these cells compared with naïve syngeneic mice, with Treg accumulation predominantly in lymphoid tissues and MDSC increased in both tumor and lymphoid tissues (Figure 4). However, functional analysis of these suppressor cell populations by *ex vivo* suppression assays showed that all tumor models induced significant activation of suppressor cells in the host (Figure 3D). CD4<sup>+</sup>CD25<sup>+</sup>FoxP3<sup>+</sup> Treg and CD11b<sup>+</sup>Gr-1<sup>high</sup>Ly6G<sup>+</sup> and CD11b<sup>+</sup>Gr-1<sup>dim</sup>Ly6G<sup>-</sup> MDSC isolated from groups of tumor-bearing mice of every model mediated significant suppression of T effector responses ( $p < 0.05$ ). While the tumor models demonstrated subtle variability in the strength of suppressor cells induced as measured by this *ex vivo* method, these data suggest that the generation of an anti-tumor immune response in any model will require overcoming the inhibitory effects of Treg and MDSC.

### Tumor-derived immunosuppressive factors ubiquitous in the tumor microenvironment

Immune dysfunction may also be induced by numerous tumor-derived factors [14,27–29,35]. Expression of *ARG-1*, *iNOS*, *TGFβ*, *IDO*, and *IL-10* genes were up-regulated most in CT26, RENCA, and 4T1 tumor specimens (Figure 1). Angiogenic and immunosuppressive genes *VEGF* and *PLGF* were present or up-regulated in all models, most significantly in those with high levels of immunogenicity (Figure 1). IHC studies further showed strong positivity for IL-6, IL-10, TGFβ, IDO, and VEGF proteins in tumor cells of all models (data not shown).

### Increased tumor-infiltrating effectors, but not suppressor cells, with progressive tumor growth

While all of the above studies evaluated the tumor-host immune interaction at a given tumor size (1cm), we also sought to understand how this interaction changed with disease progression. Four major cell populations [CTL (CD3<sup>+</sup>CD8a<sup>+</sup>CD107a<sup>+</sup>), DC (CD11c<sup>+</sup>CD80<sup>+</sup>CD86<sup>+</sup>), Treg (CD4<sup>+</sup>CD25<sup>+</sup>FoxP3<sup>+</sup>), and MDSC (CD11b<sup>+</sup>Gr-1<sup>+</sup>)] were measured in the tumor, TDLN, and spleen in groups of tumor bearing mice for each tumor model at early and late time points by flow cytometry (Supplemental Figures 3–4). Progression of the tumors *in vivo* was accompanied by increased tumor infiltration by effector cells, with the greatest change observed in the most immunogenic models (*e.g.* CT26). Interestingly, Treg and MDSC were present in secondary lymphoid tissues early in disease (5 days after subcutaneous tumor inoculation) and little change in the quantity of these peripheral populations was observed with progressive disease. These data emphasize that immune dysfunction, particularly the recruitment of immune suppressor cells, occurs early in the event of tumor progression. Furthermore, the differences in immune profiles among tumor models appeared to be inherent features of those tumor models and not a feature of differing disease stage or growth rate. In other words, more immunogenic tumor models did not begin to resemble less immunogenic tumor models with increasing tumor burden, or *vice versa*.

## Success of two immunotherapy regimens correlated directly with tumor immunogenicity

The above studies demonstrated significant variability in tumor-host immune interactions among these six transplantable tumor models and highlighted features amenable to immunotherapy in each. We hypothesized that features of these profiles could be used to guide immunotherapy selection. The presence of Treg and MDSC and the absence of mature DC and CTL in all tumor models suggested that respective inhibition and enhancement of these cells would improve anti-tumor immune responses. We further anticipated that the tumor model's pre-treatment immunogenicity level would influence response to immunotherapy regimens.

Groups of mice received no treatment (PBS vehicle only) or one of two immunotherapy regimens previously used in our laboratory (Figure 5). The first regimen (Regimen 1) consisted of tumor-targeted chemokine LEC (CCL16) to promote leukocyte tumor ingression [25,26] and low-dose chemotherapy (CTX and 5-FU) titrated to induce moderate tumor necrosis and selectively eliminate Treg and MDSC suppressor cells, respectively [36–39]. The second regimen (Regimen 2) additionally incorporated a DC tumor vaccine with toll-like receptor agonist Poly IC:LC Hiltonol [22,40]. These immunotherapy regimens were based upon previous immunotherapy studies performed in these murine models in our laboratory [41] showing good responses in some models and were selected because they incorporated components like DC vaccines, chemokine fusion proteins, and chemotherapy commonly reported in immunotherapy experiments. Of the two regimens, Regimen 2 was considered more immune stimulating and more frequently induced autoimmunity in treated animals (data not shown).

Based upon the diverse immune profiles of these six tumor models and previous immunotherapy experiments, we anticipated variable tumor response rates across models. As shown in Figure 5, CT26, RENCA, and 4T1 tumors showed the greatest positive response to both immunotherapy regimens, including significantly decreased tumor growth, increased survival, and a cure of disease in 5/10 treated CT26-bearing mice. This was followed by moderate responses in the MAD109 and LLC tumor models, which showed a statistically significant decrease in tumor growth with treatment but no difference in survival. The least immunogenic tumor model, B16 showed a poor response to these immunotherapy regimens, with only a trend toward decreased tumor growth and no difference in survival among treated and untreated groups of tumor-bearing mice. These data demonstrate that the response of established tumors in mice to these standard immunotherapy regimens correlated most to the immunogenicity of the tumor model. MHC class I expression was also shown to be an excellent surrogate marker of immunogenicity and correlated directly with response of tumor models to these immunotherapy regimens. Regimen 2 produced greater tumor regression and survival in all tumor models compared with Regimen 1, though these differences were not always statistically significant. These findings are consistent with the greater immune stimulating effects expected with Regimen 2 provided by the addition of a DC tumor vaccine and TLR agonist. This therapeutic benefit, however, is tempered by the significantly greater rate of autoimmunity observed in mice treated with this protocol, as evidenced by the generation of anti-nuclear antibodies (data not shown). Immune-related adverse events are clinically relevant challenges to immunotherapy in cancer patients and must be weighed against expected treatment benefits but also may be required to break tumor-induced immune tolerance. Pre-treatment predictors of patient response to different immunotherapy regimens, like the expression of MHC class I or immunogenicity level suggested here, will hopefully facilitate improved patient selection for cancer immunotherapy.

## DISCUSSION

Experimental tumor models are a critical pre-clinical step for the development and evaluation of immunotherapy regimens for cancer. In this study, murine tumor models were used as substitutes for human tumors and their immune escape strategies were determined and related to immunotherapy responses. Two distinct patterns of immune escape emerged from comprehensive profiling of these tumor models: 1) highly immunogenic tumors with robust activation matched by strong tumor-mediated tolerance and 2) poorly immunogenic tumors with down-regulation of antigens and evasion of host immunity. These categories are similar to those postulated by Gajewski *et al.* [42] of non-inflamed and inflamed tumor phenotypes observed in metastatic melanomas, in which poor effector cell trafficking and dominant effects of negative regulation, respectively, account for two distinct mechanisms of resistance to immune-mediated destruction of tumors. The observed tumor immunogenicity level is likely shaped by immune surveillance during tumor development [43,44] and further studies are needed to understand what drives a tumor to become poorly versus highly immunogenic. The background mouse strain (comparable to the genetic diversity among human patients) appears to impact tumor immunogenicity, with BALB/c and FVBN tumors generally more immunogenic than those syngeneic in C57BL/6, whereas the mechanism of tumor generation (*i.e.* spontaneous versus transplantable) did not consistently predict immunogenicity level. While further studies may be warranted to understand better the determinants of tumor immunogenicity, its utility as a clinical predictor of immunotherapy response is not limited by this knowledge gap. Of note, contrary to melanoma in patients, B16 melanoma model had low immunogenicity [45]. In applying pre-clinical immunotherapy results from experimental models to human cancers, translation from models with similar immune profiles may be more relevant than translation from histologically identical models.

From our studies, one key finding that emerged is that immunogenicity was the dominant feature predicting response to immunotherapy. These studies demonstrate how the immune system can be used to identify likely responders, much like Her2<sup>+</sup> status is used to select likely responders to trastuzumab therapy. Immunotherapy has lagged significantly in the educated application of tumor bioprofile information for the selection of treatment approaches in patients that are often assigned to immunotherapy clinical trial groups based only on disease stage or histology. Sporadic successes in tumor immunotherapy trials suggest that traditional patient stratifiers are of limited utility in predicting response to this newer modality [3,7,42]. For translation to patients, use of select immune markers to predict immunotherapy response is an important feasibility hurdle. These studies found MHC class I expression on tumor cells to be a singular predictor of the overall tumor immunogenicity level, and by extension, a predictor of response to two immunotherapy regimens. Previous reports in mice using other immunotherapy regimens, namely B7 and OX40 agonists, also correlated high tumor immunogenicity with greater tumor response [46,47]. Examination of immune profiles in human head and neck cancers performed recently in our laboratory suggests that MHC class I expression may be a correlate of immunogenicity and immune escape strategy in some human cancers as well [42]. Similarly, in patients with colorectal cancer, an inflamed phenotype before treatment more likely corresponded to patient responses to tumor vaccine strategies, including DC vaccination, MAGE-A3 protein vaccination, and multi-tumor antigen vaccination with IL-12 [42,48–50]. A systematic review by Lima *et al.* [51] identified a significant association between strong tumor MHC class I expression and improved response to Bacillus Calmette-Guerin (BCG) vaccine immunotherapy in patients with bladder cancer. In addition to overall MHC class I expression, it is important to acknowledge that MHC haplotype has also been shown to correlate with immunotherapy response, particularly in the setting of tumor vaccines. While not addressed in this study, differences in MHC haplotype influence the strength of anti-

tumor immune responses and are an important consideration in human trials. Furthermore, additional biomarkers to predict immunotherapy response should be sought. Lima *et al.* [51] also found that a high frequency of tumor-infiltrating CD68<sup>+</sup> cells, or tumor-associated macrophages, was associated with a poor response to BCG immunotherapy in bladder cancer patients. Wantanabe *et al.* [52] reported that increased levels of cytokines, including IL-2, IL-6, IL-8, IL-10, and tumor necrosis factor- $\alpha$ , correlated with a better clinical response to BCG vaccination in bladder cancer patients. In melanoma patients, clinical response to immunotherapy by CTLA-4 blockade with monoclonal antibody ipilimumab is associated with high baseline levels of FoxP3, expressed by immunosuppressive regulatory T cells, and immunosuppressive enzyme IDO [53]. Tumor vasculature permeability to immunotherapy reagents and effector cells is another potential predictor for treatment response, as augmentation of these characteristics has yielded improved immunotherapy responses [25,26,54]. Serum analytes, such as IFN $\gamma$  inducible protein 10 and CXCL10, are another promising set of biomarkers for predicting immunotherapy response and may be preferable in patients with non-operable cancers [55,56]. Given the multitude of immunotherapy regimens now available and the risks associated with any immunotherapy treatment, pretreatment tumor characteristics predicting good clinical response to therapy will be valuable and additional studies in this area are warranted.

Another consideration in immune profiling cancers by tumor specimen biopsy is that primary and peripheral tumor sites may display different levels of immunogenicity. In clinical practice, often only the primary tumor specimen and nearby lymph node metastasis specimens may be available for immune profiling. For cancers in which tumors are not routinely resected, it is possible that only limited diagnostic biopsy specimens would be available for profiling. It remains unclear the extent to which human cancers vary amongst primary and metastatic or recurrent lesions with regard to expression of these immune markers, and future studies are needed to adequately address that question. Based upon our findings in this study, we would recommend that therapy be titrated to the least immunogenic parts of the tumor if the goal is cure of disease. The known risk with overly robust immunotherapy treatment is induction of autoimmunity, which in cases like thyroiditis, may be a tolerable side effect for cancer patients. One goal of assigning a highly immunogenic or poorly immunogenic label to cancers is to reduce the incidence of undertreating poorly immunogenic tumors and overtreating highly immunogenic tumors, as the likely outcomes of these mismatches are unsuccessful treatment and autoimmunity, respectively. Obtaining comprehensive immune profile information for a cancer in a way that is readily available in the clinical setting remains a challenge.

We suggest that strong or poor tumor immunogenicity is a predictor of responses to some forms of immunotherapy and that this or other discrete features of the immune profile can be used to predict responses to immunotherapy. In addition, as shown in Table I, comprehensive immune profiling of murine tumor models may therefore be used to identify specific immune deficits and therapeutic targets. One example is the results obtained by Murphy *et al.* [22] who showed that murine glioblastoma tumors that lack OX40L expression were successfully treated with Fc- $\mu$ OX40L immunotherapy. The correlation of immunotherapy response with MHC class I expression suggests that therapies to increase tumor antigen expression are likely to be efficacious in immune competent hosts by bolstering endogenous immune activation and cell-mediated tumor killing. This is consistent with reports of improved anti-tumor T-cell responses and tumor regression when immunotherapy is directly preceded by radiation therapy or chemotherapy in murine models [57–59]. For tumors in which tumor antigen presentation appears to be sufficient, the greatest benefit may result from enhancement of anti-tumor T-cell activity or numbers (*e.g.* infusion of engineered T-cells) and inhibition of tumor-mediated suppression (*e.g.* Treg and MDSC inhibition). Lastly, the deficit of tumor-infiltrating effector cells seen in all tumor

models highlights the need for therapies that alter the tumor vasculature and immune cell trafficking patterns to promote tumor ingression like that seen with targeted LEC therapy [25,26]. Collectively these data demonstrate the value of selective immune profiling of tumors as a means not only to understanding immune escape and identifying new therapeutic targets, but to predict immunotherapy response in patients.

## Supplementary Material

Refer to Web version on PubMed Central for supplementary material.

## Acknowledgments

The authors thank Dr. Andres Salazar for providing Hiltonol, James Pang for assistance with transplantable tumor model experimental animals, Falvia E. Popescu for providing the FVBN spontaneous and transplanted samples, and Christopher Roque for help with the flow cytometry analyses. This work was supported in part by the USC Institute for Innovation Ideas Empowered Program, NIH grants 3T32GM067587-07S1 (M.G.L.), DOD grant W81XWH-11-1-0466, and Cancer Therapeutic Laboratories, Inc. (Los Angeles, CA).

## REFERENCES

1. Gooden MJ, de Bock GH, Leffers N, Daemen T, Nijman HW. The prognostic influence of tumour-infiltrating lymphocytes in cancer: a systematic review with meta-analysis. *Br J Cancer*. 2011; 105(1):93–103. [PubMed: 21629244]
2. Russell SM, Angell TE, Lechner MG, Liebertz DJ, Correa AJ, Sinha UK, Kokot N, Epstein AL. Immune Cell Infiltration Patterns and Survival in Head and Neck Squamous Cell Carcinoma. *Head and Neck Oncology*. Feb 27.2013 5(3):24.
3. Galon J, Pagès F, Marincola FM, Thurin M, Trinchieri G, Fox BA, Gajewski TF, Ascierto PA. The immune score as a new possible approach for the classification of cancer. *J Transl Med*. 2012; 10:1. [PubMed: 22214470]
4. Stewart TJ, Smyth MJ. Improving cancer immunotherapy by targeting tumor-induced immune suppression. *Cancer Metastasis Rev*. 2011; 30(1):125–140. [PubMed: 21249424]
5. Gajewski TF, Louahed J, Brichard VG. Gene signature in melanoma associated with clinical activity: a potential clue to unlock cancer immunotherapy. *Cancer J*. 2010; 16(4):399–403. [PubMed: 20693853]
6. May KF Jr, Gulley JL, Drake CG, Dranoff G, Kantoff PW. Prostate cancer immunotherapy. *Clin Cancer Res*. 2011; 17(16):5233–5238. [PubMed: 21700764]
7. Lechner MG, Russell SM, Bass RS, Epstein AL. Chemokines, costimulatory molecules and fusion proteins for the immunotherapy of solid tumors. *Immunotherapy*. 2011; 3(11):1317–1340. [PubMed: 22053884]
8. Callahan MK, Wolchok JD, Allison JP. Anti-CTLA-4 antibody therapy: immune monitoring during clinical development of a novel immunotherapy. *Semin Oncol*. 2010; 37(5):473–484. [PubMed: 21074063]
9. Di Giacomo AM, Biagioli M, Maio M. The emerging toxicity profiles of anti-CTLA-4 antibodies across clinical indications. *Semin Oncol*. 2010; 37(5):499–507. [PubMed: 21074065]
10. Shablak A, Sikand K, Shanks JH, Thistlethwaite F, Spencer-Shaw A, Hawkins RE. High-dose interleukin-2 can produce a high rate of response and durable remissions in appropriately selected patients with metastatic renal cancer. *J Immunother*. 2011; 34(1):107–112. [PubMed: 21150719]
11. McDermott DF. Improving the therapeutic index of IL-2. *Clin Adv Hematol Oncol*. 2010; 8(12): 862–864. [PubMed: 21326162]
12. Kirkwood JM, Tarhini AA. Biomarkers of therapeutic response in melanoma and renal cell carcinoma: potential inroads to improved immunotherapy. *J Clin Oncol*. 2009; 27(16):2583–2585. [PubMed: 19364958]
13. Mlecnik B, Bindea G, Pagès F, Galon J. Tumor immunosurveillance in human cancers. *Cancer Metastasis Rev*. 2011; 30(1):5–12. [PubMed: 21249426]

14. Stewart TJ, Abrams SI. How tumours escape mass destruction. *Oncogene*. 2008; 27(45):5894–5903. [PubMed: 18836470]
15. Garcia-Lora A, Algarra I, Garrido F. MHC class I antigens, immune surveillance, and tumor immune escape. *J Cell Physiol*. 2003; 195(3):346–355. [PubMed: 12704644]
16. Du C, Wang Y. The immunoregulatory mechanisms of carcinoma for its survival and development. *J Exp Clin Cancer Res*. 2011; 30:12. [PubMed: 21255410]
17. Sadun RE, Sachsman SM, Chen X, Christenson KW, Morris WZ, Hu P, Epstein AL. Immune signatures of murine and human cancers reveal unique mechanisms of tumor escape and new targets for cancer immunotherapy. *Clin Cancer Res*. 2007; 13(13):4016–4025. [PubMed: 17606736]
18. Schaer DA, Lesokhin AM, Wolchok JD. Hiding the road signs that lead to tumor immunity. *J Exp Med*. 2011; 208(10):1937–1940. [PubMed: 21948803]
19. Fridman WH, Galon J, Pagès F, Tartour E, Sautès-Fridman C, Kroemer G. Prognostic and predictive impact of intra- and peritumoral immune infiltrates. *Cancer Res*. 2011; 71(17):5601–5605. [PubMed: 21846822]
20. Galon J, Costes A, Sanchez-Cabo F, Kirilovsky A, Mlecnik B, Lagorce-Pagès C, Tosolini M, Camus M, Berger A, Wind P, Zinzindohoué F, Bruneval P, Cugnenc PH, Trajanoski Z, Fridman WH, Pagès F. Type, density, and location of immune cells within human colorectal tumors predict clinical outcome. *Science*. 2006; 313(5795):1960–1964. [PubMed: 17008531]
21. Lechner MG, Megiel C, Russell SM, Bingham B, Arger N, Woo T, Epstein AL. Functional characterization of human Cd33+ and Cd11b+ myeloid-derived suppressor cell subsets induced from peripheral blood mononuclear cells co-cultured with a diverse set of human tumor cell lines. *J Transl Med*. 2011; 9:90. [PubMed: 21658270]
22. Murphy KA, Lechner MG, Popescu FE, Bedi J, Decker SA, Hu P, Erickson JR, O'Sullivan MG, Swier L, Salazar AM, Olin MR, Epstein AL, Ohlfest JR. An in vivo immunotherapy screen of costimulatory molecules identifies Fc-OX40L as a potent reagent for the treatment of established murine gliomas. *Clin Cancer Res*. 2012; 18(17):4657–4668. [PubMed: 22781551]
23. Wiesner SM, Decker SA, Larson JD, Ericson K, Forster C, Gallardo JL, Long C, Demorest ZL, Zamora EA, Low WC, SantaCruz K, Largaespada DA, Ohlfest JR. De novo induction of genetically engineered brain tumors in mice using plasmid DNA. *Cancer Res*. 2009; 69(2):431–439. [PubMed: 19147555]
24. Russell SM, Lechner MG, Gong L, Megiel C, Liebertz DJ, Masood R, Correa AJ, Han J, Puri RK, Sinha UK, Epstein AL. USC-HN2, a new model cell line for recurrent oral cavity squamous cell carcinoma with immunosuppressive characteristics. *Oral Oncol*. 2011; 47(9):810–817. [PubMed: 21719345]
25. Li J, Hu P, Khawli LA, Epstein AL. LEC/chTNT-3 fusion protein for the immunotherapy of experimental solid tumors. *J Immunother*. 2003; 26(4):320–331. [PubMed: 12843794]
26. Li J, Hu P, Khawli LA, Epstein AL. Complete regression of experimental solid tumors by combination LEC/chTNT-3 immunotherapy and CD25(+) T-cell depletion. *Cancer Res*. 2003; 63(23):8384–8392. [PubMed: 14679000]
27. Katz JB, Muller AJ, Prendergast GC. Indoleamine 2,3-dioxygenase in T-cell tolerance and tumoral immune escape. *Immunol Rev*. 2008; 222:206–221. [PubMed: 18364004]
28. Condamine T, Gabrilovich DI. Molecular mechanisms regulating myeloid-derived suppressor cell differentiation and function. *Trends Immunol*. 2011; 32(1):19–25. [PubMed: 21067974]
29. Mocellin S, Wang E, Marincola FM. Cytokines and immune response in the tumor microenvironment. *J Immunother*. 2001; 24(5):392–407.
30. Ostrand-Rosenberg S. Animal models of tumor immunity, immunotherapy and cancer vaccines. *Curr Opin Immunol*. 2004; 16(2):143–150. [PubMed: 15023405]
31. von Bergwelt-Baildon MS, Vonderheide RH, Maecker B, Hirano N, Anderson KS, Butler MO, et al. Human primary and memory cytotoxic T lymphocyte responses are efficiently induced by means of CD40-activated B cells as antigen-presenting cells: potential for clinical application. *Blood*. 2002; 99(9):3319–3325. [PubMed: 11964299]
32. Lynch DH. The promise of 4-1BB (CD137)-mediated immunomodulation and the immunotherapy of cancer. *Immunol Rev*. 2008; 222:277–286. [PubMed: 18364008]

33. Jensen SM, Maston LD, Gough MJ, Ruby CE, Redmond WL, Crittenden M, Li Y, Puri S, Poehlein CH, Morris N, Kovacs-Bankowski M, Moudgil T, Twitty C, Walker EB, Hu HM, Urba WJ, Weinberg AD, Curti B, Fox BA. Signaling through OX40 enhances antitumor immunity. *Semin Oncol.* 2010; 37(5):524–532. [PubMed: 21074068]
34. Placke T, Kopp HG, Salih HR. Glucocorticoid-induced TNFR-related (GITR) protein and its ligand in antitumor immunity: functional role and therapeutic modulation. *Clin Dev Immunol.* 2010; 2010:239083. [PubMed: 20936139]
35. Lechner MG, Liebertz DJ, Epstein AL. Characterization of cytokine-induced myeloid-derived suppressor cells from normal human peripheral blood mononuclear cells. *J Immunol.* 2010; 185(4):2273–2284. [PubMed: 20644162]
36. Ghiringhelli F, Menard C, Puig PE, Ladoire S, Roux S, Martin F, Solary E, Le Cesne A, Zitvogel L, Chauffert B. Metronomic cyclophosphamide regimen selectively depletes CD4+CD25+ regulatory T cells and restores T and NK effector functions in end stage cancer patients. *Cancer Immunol Immunother.* 2007; 56(5):641–648. [PubMed: 16960692]
37. Zhao J, Cao Y, Lei Z, Yang Z, Zhang B, Huang B. Selective depletion of CD4+CD25+ Foxp3+ regulatory T cells by low-dose cyclophosphamide is explained by reduced intracellular ATP levels. *Cancer Res.* 2010; 70(12):4850–4858. [PubMed: 20501849]
38. Lechner, MGm; Epstein, AL. A new mechanism for blocking myeloid-derived suppressor cells by CpG. *Clin Cancer Res.* 2011; 17(7):1645–1648. [PubMed: 21288925]
39. Vincent J, Mignot G, Chalmin F, Ladoire S, Bruchard M, Chevriaux A, Martin F, Apetoh L, Rébé C, Ghiringhelli F. 5-Fluorouracil selectively kills tumor-associated myeloid-derived suppressor cells resulting in enhanced T cell-dependent antitumor immunity. *Cancer Res.* 2010; 70:3052–3061. [PubMed: 20388795]
40. Salazar AM, Levy HB, Ondra S, Kende M, Scherokman B, Brown D, Mena H, Martin N, Schwab K, Donovan D, Dougherty D, Pulliam M, Ippolito M, Graves M, Brown H, Ommaya A. Long-term treatment of malignant gliomas with intramuscularly administered polyinosinic-polycytidylic acid stabilized with polylysine and carboxymethylcellulose: an open pilot study. *Neurosurgery.* 1996; 38(6):1096–1103. [PubMed: 8727138]
41. Lechner, MG. Human myeloid-derived suppressor cells in cancer: induction, functional characterization, and therapy. Thesis dissertation, University of Southern California, Department of Pathology of the Keck School of Medicine; 2011.
42. Gajewski TF, Fuertes M, Spaapen R, Zheng Y, Kline J. Molecular profiling to identify relevant immune resistance mechanisms in the tumor microenvironment. *Curr Opin Immunol.* 2011; 23(2): 286–292. [PubMed: 21185705]
43. Schreiber RD, Old LJ, Smyth MJ. Cancer immunoediting: integrating immunity's roles in cancer suppression and promotion. *Science.* 2011; 331(6024):1565–1570. [PubMed: 21436444]
44. Shankaran V, Ikeda H, Bruce AT, White JM, Swanson PE, Old LJ, Schreiber RD. IFN $\gamma$  and lymphocytes prevent primary tumour development and shape tumour immunogenicity. *Nature.* 2001; 410(6832):1107–1111. [PubMed: 11323675]
45. Zeiser R, Schnitzler M, Andrlova H, Hellige T, Meiss F. Immunotherapy for malignant melanoma. *Curr Stem Cell Res Ther.* 2012; 7(3):217–228. [PubMed: 22329580]
46. Kjaergaard J, Tanaka J, Kim JA, Rothchild K, Weinberg A, Shu S. Therapeutic efficacy of OX-40 receptor antibody depends on tumor immunogenicity and anatomic site of tumor growth. *Cancer Res.* 2000; 60(19):5514–5521. [PubMed: 11034096]
47. Chen L, McGowan P, Ashe S, Johnston J, Li Y, Hellström I, Hellström KE. Tumor immunogenicity determines the effect of B7 costimulation on T cell-mediated tumor immunity. *J Exp Med.* 1994; 179(2):523–532. [PubMed: 7507508]
48. Gajewski, TF.; Meng, Y.; Harlin, H. Chemokines expressed in melanoma metastases associated with T cell infiltration. *J Clin Oncol; ASCO Annual Meeting Proceedings Part I; 2007.* p. 8501
49. Gajewski TF, Zha Y, Thurner B, Schuler G. Association of gene expression profile in melanoma and survival to a dendritic cell-based vaccine. *J Clin Oncol.* 2009; 27(15S):9002.
50. Louahed J, Gruselle O, Gaulis S, Coche T, Eggermont AM, Kruit W, Dreno B, Chiarion Sileni V, Lehmann F, Brichard VG. Expression of defined genes identified by pre-treatment tumor

- profiling: association with clinical responses to the GSK MAGE-A3 immunotherapeutic in metastatic melanoma patients. *J Clin Oncol.* 2008; 26(suppl):9045.
51. Lima L, Dinis-Ribeiro M, Longatto-Filho A, Santos L. Predictive biomarkers of bacillus calmette-guérin immunotherapy response in bladder cancer: where are we now? *Adv Urol.* 2012; 2012:232609. [PubMed: 22919375]
  52. Watanabe E, Matsuyama H, Matsuda K, Ohmi C, Tei Y, Yoshihiro S, Ohmoto Y, Naito K. Urinary interleukin-2 may predict clinical outcome of intravesical bacillus Calmette-Guérin immunotherapy for carcinoma in situ of the bladder. *Cancer Immunol Immunother.* 2003; 52(8): 481–486. [PubMed: 12707736]
  53. Hoos A, Ibrahim R, Korman A, Abdallah K, Berman D, Shahabi V, Chin K, Canetta R, Humphrey R. Development of ipilimumab: contribution to a new paradigm for cancer immunotherapy. *Semin Oncol.* 2010; 37(5):533–546. [PubMed: 21074069]
  54. LeBerthon B, Khawli LA, Alauddin M, Miller GK, Charak BS, Mazumder A, Epstein AL. Enhanced tumor uptake of macromolecules induced by a novel vasoactive interleukin 2 immunoconjugate. *Cancer Res.* 1991; 51(10):2694–2698. [PubMed: 2021947]
  55. Schwaab T, Schwarzer A, Wolf B, Crocenzi TS, Seigne JD, Crosby NA, Cole BF, Fisher JL, Uhlenhake JC, Mellinger D, Foster C, Szczepiorkowski ZM, Webber SM, Schned AR, Harris RD, Barth RJ Jr, Heaney JA, Noelle RJ, Ernstoff MS. Clinical and immunologic effects of intranodal autologous tumor lysate-dendritic cell vaccine with Aldesleukin (Interleukin 2) and IFN- $\alpha$ 2a therapy in metastatic renal cell carcinoma patients. *Clin Cancer Res.* 2009; 15(15):4986–4992. [PubMed: 19622576]
  56. Okada H, Kalinski P, Ueda R, Hoji A, Kohanbash G, Donegan TE, Mintz AH, Engh JA, Bartlett DL, Brown CK, Zeh H, Holtzman MP, Reinhart TA, Whiteside TL, Butterfield LH, Hamilton RL, Potter DM, Pollack IF, Salazar AM, Lieberman FS. Induction of CD8<sup>+</sup> T-cell responses against novel glioma-associated antigen peptides and clinical activity by vaccinations with  $\alpha$ -type 1 polarized dendritic cells and polyinosinic-polycytidylic acid stabilized by lysine and carboxymethylcellulose in patients with recurrent malignant glioma. *J Clin Oncol.* 2011; 29(3): 330–336. [PubMed: 21149657]
  57. Yokouchi H, Yamazaki K, Chamoto K, Kikuchi E, Shinagawa N, Oizumi S, Hommura F, Nishimura T, Nishimura M. Anti-OX40 monoclonal antibody therapy in combination with radiotherapy results in therapeutic antitumor immunity to murine lung cancer. *Cancer Sci.* 2008; 99(2):361–367. [PubMed: 18201271]
  58. Gough MJ, Crittenden MR, Sarff M, Pang P, Seung SK, Vetto JT, Hu HM, Redmond WL, Holland J, Weinberg AD. Adjuvant therapy with agonistic antibodies to CD134 (OX40) increases local control after surgical or radiation therapy of cancer in mice. *J Immunother.* 2010; 33(8):798–809. [PubMed: 20842057]
  59. Hirschhorn-Cymerman D, Rizzuto GA, Merghoub T, Cohen AD, Avogadri F, Lesokhin AM, Weinberg AD, Wolchok JD, Houghton AN. OX40 engagement and chemotherapy combination provides potent antitumor immunity with concomitant regulatory T cell apoptosis. *J Exp Med.* 2009; 206(5):1103–1116. [PubMed: 19414558]

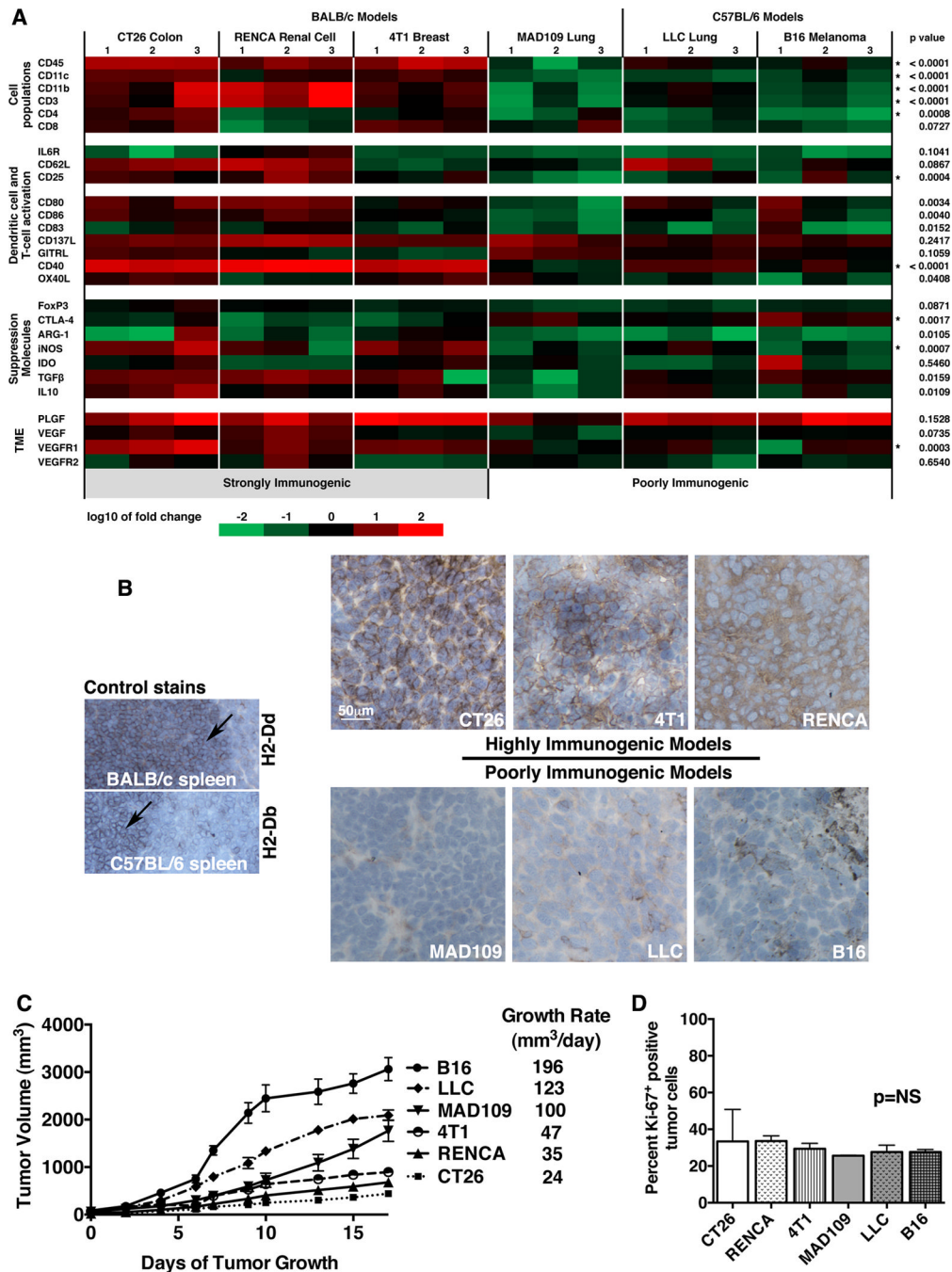


**Figure 1. Variable immunogenicity levels observed among murine solid tumor models in vivo**  
**A**, Intratumoral immune-related gene as measured by qRT-PCR techniques in fresh frozen tumor specimens. Gene expression shown as log10 of mean fold change relative to syngeneic naïve controls with significant differences between highly and poorly immunogenic models indicated by an asterisk. **B**, IHC showing MHC class I molecule H2-Dd (BALB/c) or H2-Db (C57BL/6) expression in tumor models (400× orig. mag.). **C**, Variable *in vivo* growth rates of six tumor models in immunocompetent mice (n=5). **D**, No significant differences observed in mean (n=3) Ki-67 positivity per 100 tumor cells as determined by IHC.

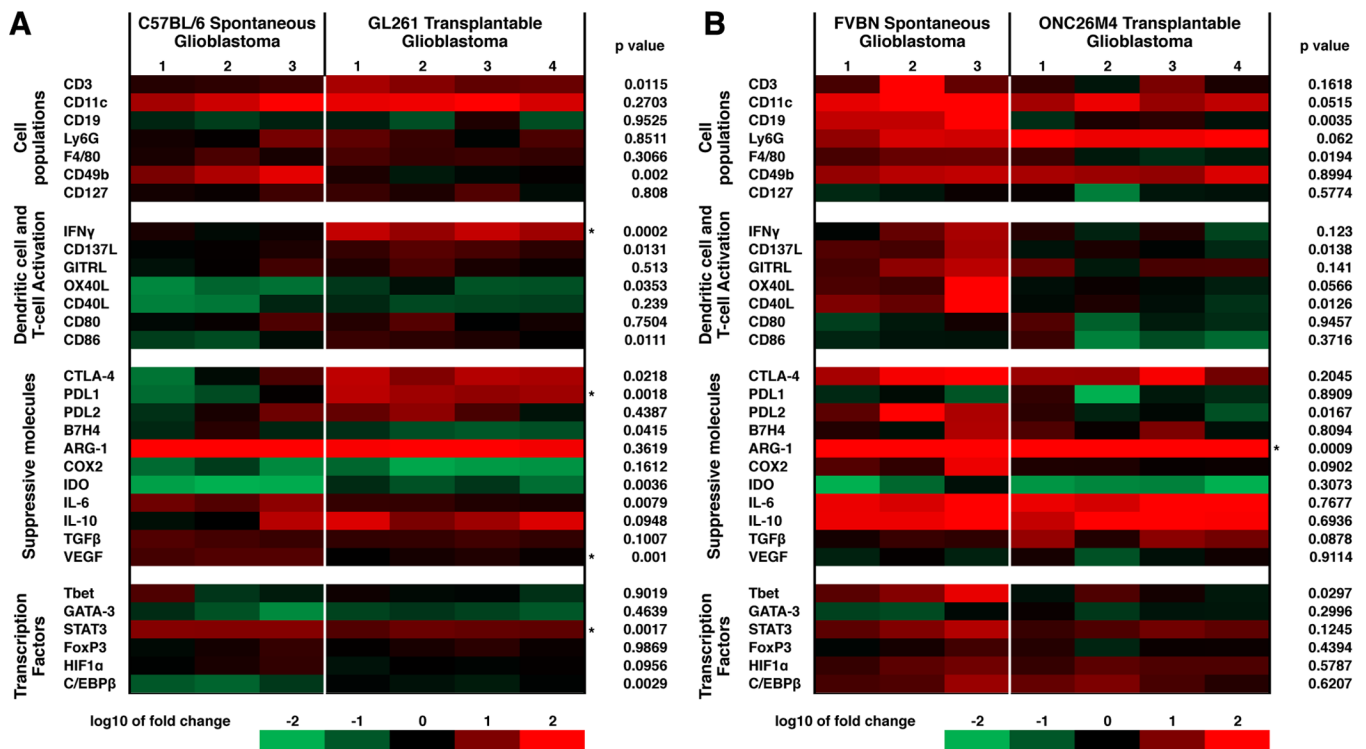


**Figure 2. Few differences in intratumoral immune-related gene expression between transplantable and spontaneous glioblastoma tumor models in C57BL/6 (A) and FVB (B) mice** Gene expression shown as log<sub>10</sub> of fold change relative to expression levels in syngeneic naïve controls; mean shown with SEM (n = 3). Genes with significantly different expression between spontaneous and transplantable models are indicated by an asterisk with corresponding p-values.

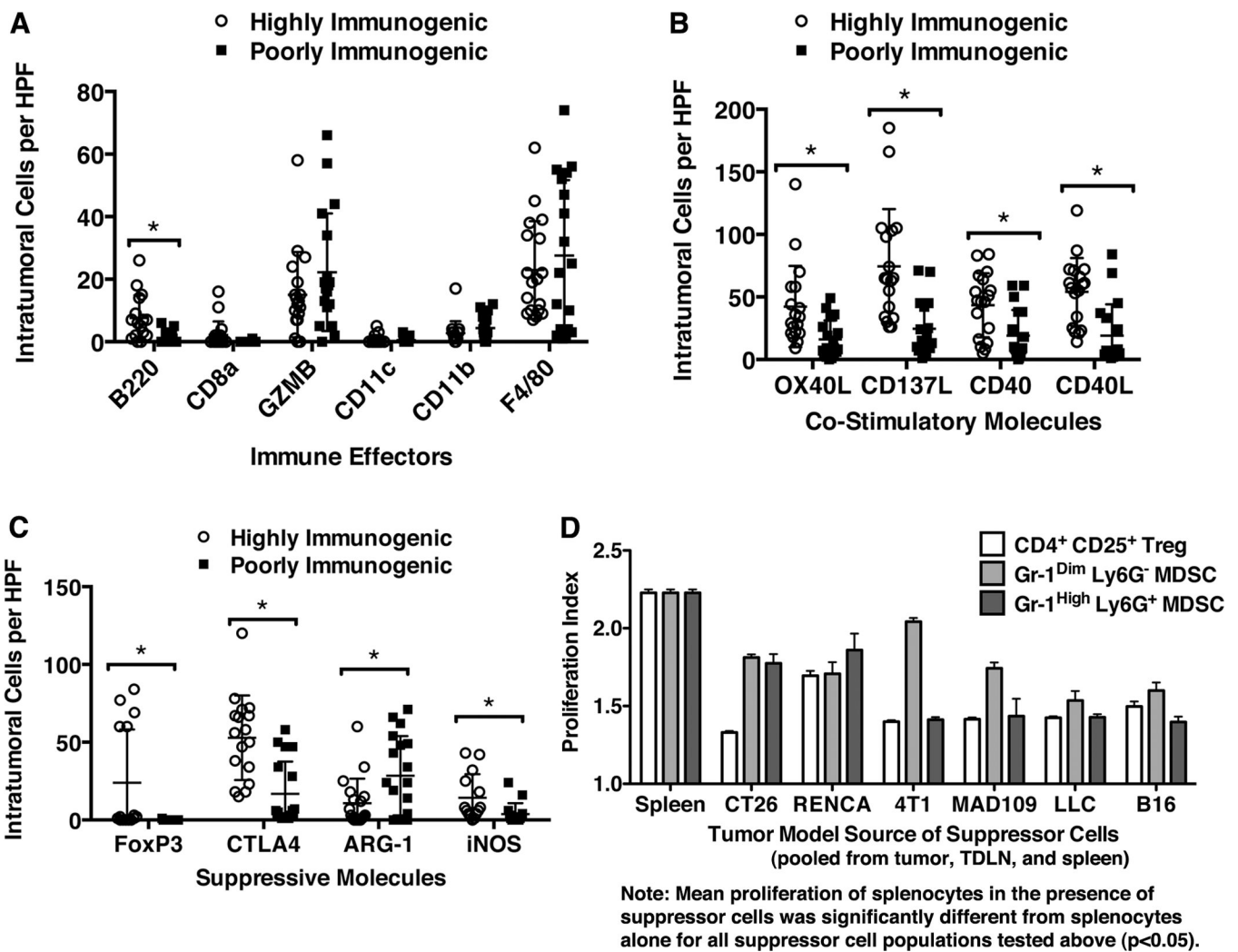


**Figure 3. Differences in intratumoral B cells, co-stimulatory ligands, and suppressive molecules with tumor immunogenicity, but consistent absence of CTL or DC and presence of suppressor cells**

Measurement of tumor-infiltrating immune effectors (A) and expression of co-stimulatory ligands (B) and suppressive molecules (C) on TIL by IHC. Markers showing significantly different positivity on TIL between highly (CT26, 4T1, RENCA) and poorly (MAD109, LLC, B16) immunogenic models are indicated by an asterisk. D, *Ex vivo* functional evaluations of Treg and MDSC suppressor cells isolated from groups (n=3) of tumor-bearing mice. 1:4 ratio of suppressor cells to responder T cells. All examined suppressor cell populations in all tumor models produced significant suppression of splenocyte proliferation (p<0.05).

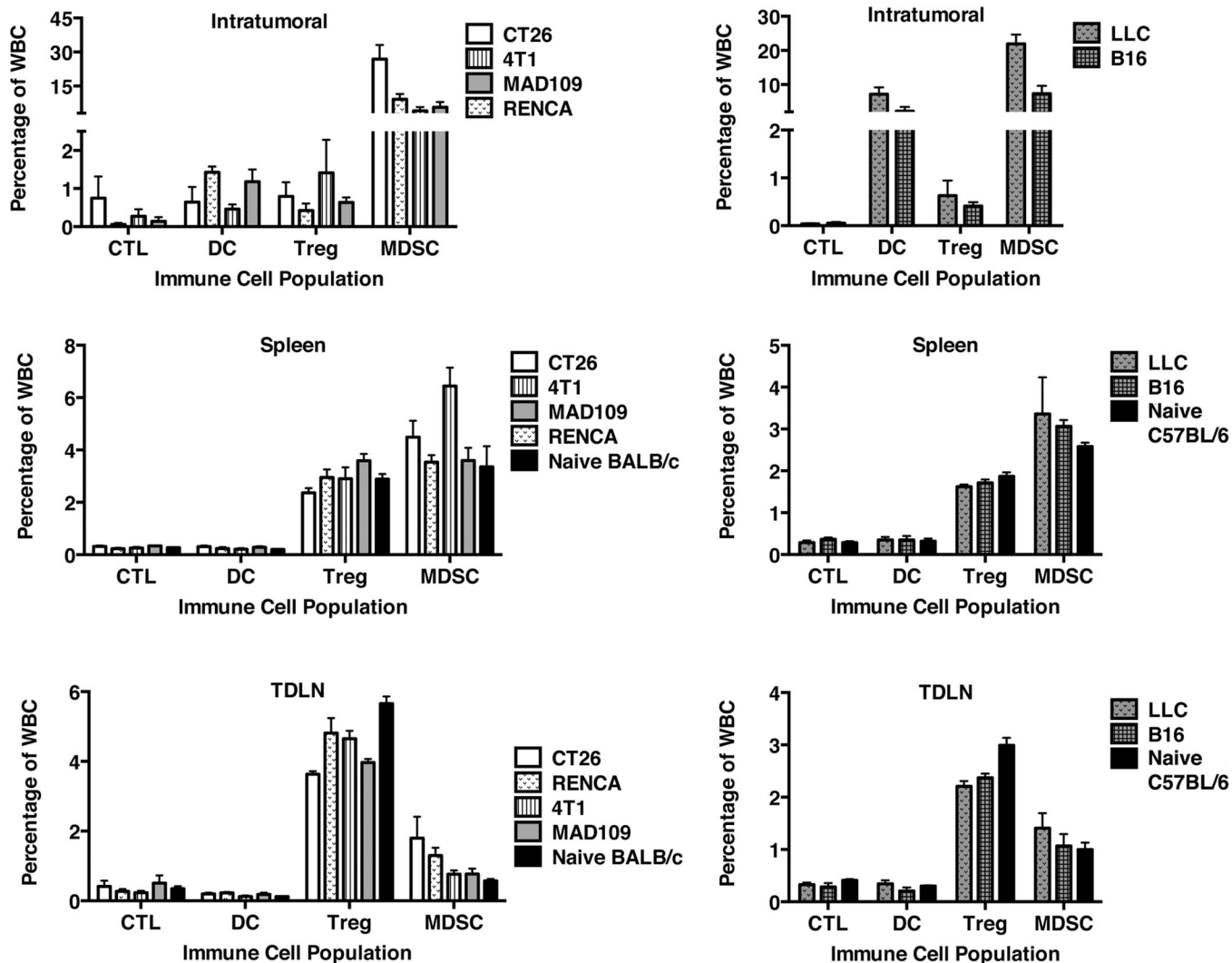


**Figure 4. FACS analysis demonstrating a notable absence of effector cells in the tumor and draining lymphoid tissues but strong presence of suppressor cells in all models**  
 Shown is the mean percentage of positive leukocytes for CTL, DC, Treg, and MDSC markers measured in each tissue by flow cytometry techniques (n=4).

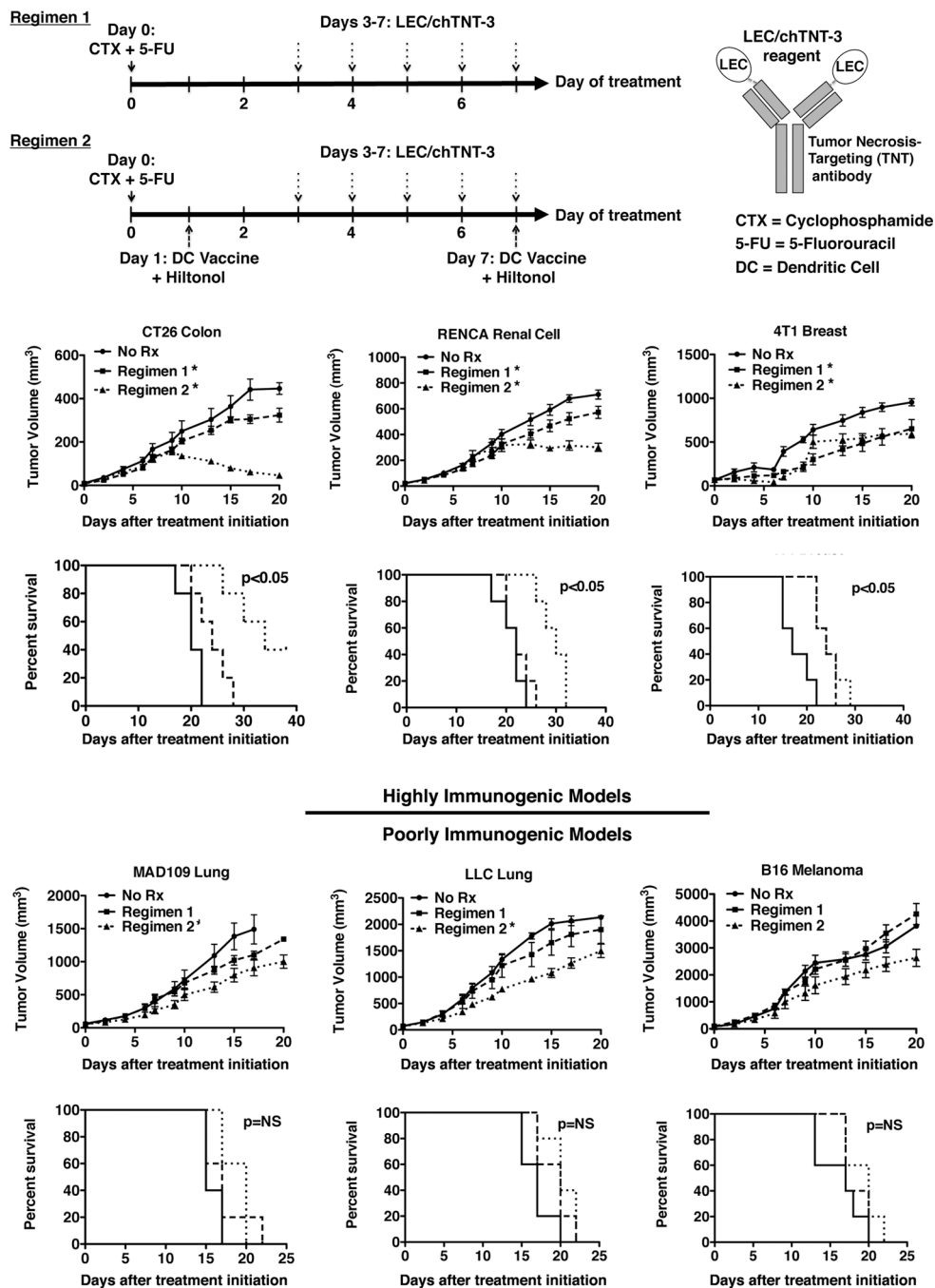


**Figure 5. Response to immunotherapy in six murine tumor models correlated with immunogenicity**

Tumor volume and survival were evaluated in groups (n=5) of tumor-bearing mice receiving no treatment or two immunotherapy regimens. Significant differences in mean tumor volume at day 17 between treatment group and untreated controls indicated by an asterisk. Groups of CT26, RENCA, and 4T1-bearing mice receiving immunotherapy regimens had significantly longer survival than controls (p<0.05).

**Table I**

## Immunotherapy approaches suggested by immune profiles of murine tumor models

<b>Approaches applicable to many tumor models</b>	<p>Activation of tumor-targeted CD8<sup>+</sup> T-cells (e.g. engineered T-cells, vaccines)</p> <p>Increased tumor trafficking of antigen presenting and effector cells in tumor microenvironment (e.g. TLR agonists, dendritic cell vaccines, targeted chemokines)</p> <p>Inhibition of suppressor cell anti-tumor effects (e.g. regulatory T cell or myeloid-derived suppressor cell inhibition)</p>
<b>CT26 Colon</b>	<p>PLGF and VEGF inhibition</p> <p>Regulatory T cell inhibition or depletion</p> <p>TGFβ blockade</p> <p>CTLA-4 inhibition on TIL</p> <p>iNOS inhibition</p>
<b>RENCA Renal Cell</b>	<p>CD4<sup>+</sup> and CD8<sup>+</sup> T-cell tumor ingression</p> <p>Co-stimulation with GITRL, CD40/CD40L, and OX40L fusion proteins</p> <p>TGFβ blockade</p> <p>CTLA-4 inhibition on TIL</p> <p>PLGF and VEGF inhibition</p>
<b>4T1 Breast</b>	<p>Co-stimulation with GITRL and OX40L fusion proteins</p> <p>Regulatory T cell inhibition or depletion</p> <p>Myeloid-derived suppressor cell inhibition or depletion</p> <p>CTLA-4 inhibition on TIL</p>
<b>MAD109 Lung</b>	<p>Co-stimulation with CD40 and OX40L fusion proteins</p> <p>ARG-1 inhibition and myeloid-derived suppressor cell inhibition or depletion</p> <p>CTLA-4 blockade on tumor cells and on TIL</p> <p>Increase tumor antigen expression (IFNγ)</p>
<b>LLC Lung</b>	<p>Stimulation with co-stimulatory fusion proteins (GITRL, CD40, OX40L, CD137L)</p> <p>ARG-1 inhibition</p> <p>CTLA-4 blockade on tumor cells</p> <p>Increase tumor antigen expression (IFNγ)</p>
<b>B16 Melanoma</b>	<p>Stimulation with co-stimulatory fusion proteins (GITRL, CD40, OX40L, CD137L)</p> <p>CTLA-4 blockade on tumor cells</p> <p>Increase tumor antigen expression (IFNγ)</p>
<b>ONC26M4 Glioblastoma</b>	<p>CTLA-4 and B7-H4 blockade</p> <p>Stimulation with co-stimulatory fusion proteins (GITRL, CD40, OX40L, CD137L)</p> <p>ARG-1 inhibition</p> <p>IL-6 and IL-10 blockade</p> <p>STAT3 inhibition</p> <p>Countering tumor hypoxia and HIF1α signaling</p>
<b>GL261 Glioblastoma</b>	<p>CTLA-4, PDL1, and PDL2 blockade</p> <p>Stimulation with co-stimulatory fusion proteins (GITRL, CD40, OX40L, CD137L)</p> <p>ARG-1 inhibition</p> <p>IL-10 blockade</p> <p>STAT3 inhibition</p>